

1 **Rapidly increasing sulfate concentration: a hidden promoter of eutrophication in**  
2 **shallow lakes**

3 Chuanqiao Zhou<sup>a,1</sup>, Yu Peng<sup>a,1</sup>, Li Chen<sup>a</sup>, Miaotong Yu<sup>a</sup>, Muchun Zhou<sup>b</sup>, Runze Xu<sup>a</sup>,  
4 Lanqing Zhang<sup>a</sup>, Siyuan Zhang<sup>c</sup>, Xiaoguang Xu<sup>a,\*</sup>, Limin Zhang<sup>a</sup>, Guoxiang Wang<sup>a</sup>

5 <sup>a</sup> School of Environment, Nanjing Normal University, Jiangsu Center for Collaborative  
6 Innovation in Geographical Information Resource Development and Application,  
7 Jiangsu Key Laboratory of Environmental Change and Ecological Construction,  
8 Nanjing 210023, China

9 <sup>b</sup> China Aerospace Science and Industry Nanjing Chenguang group, Nanjing 210022,  
10 China

11 <sup>c</sup> School of Energy and Environment, Southeast University, Nanjing 210096, China

12 *\*Corresponding author: 1, Wenyuan Road, Xianlin University District, Nanjing,*  
13 *210023, China*

14 *E-mail address: [xxg05504118@163.com](mailto:xxg05504118@163.com)*

15 <sup>1</sup> Both authors contributed equally

16 **Keywords:** Sulfate reduction; iron reduction; phosphorus release; eutrophication;  
17 sulfate reduction bacteria

18 **Abstract:**

19 Except for excessive nutrient input and climate warming, the rapidly rising  $\text{SO}_4^{2-}$   
20 concentration is considered as a crucial contributor to the eutrophication in shallow  
21 lakes, however, the driving process and mechanism are still far from clear. In this study,  
22 we constructed a series of microcosms with initial  $\text{SO}_4^{2-}$  concentrations of 0, 30, 60, 90,

23 120 and 150 mg/L to simulate the rapidly  $\text{SO}_4^{2-}$  increase of Lake Taihu subjected to  
24 cyanobacteria blooms. Results showed that the sulfate reduction rate was stimulated by  
25 the increase of initial  $\text{SO}_4^{2-}$  concentrations and cyanobacteria-derived organic matter,  
26 with the maximal sulfate reduction rate of 39.68 mg/L·d in the treatment of 150 mg/L  
27  $\text{SO}_4^{2-}$  concentration. During the sulfate reduction, the produced maximal  $\Sigma\text{S}^{2-}$   
28 concentration in the overlying water and acid volatile sulfate (AVS) in the sediments  
29 were 3.15 mg/L and 11.11 mg/kg, respectively, and both of them were positively  
30 correlated with initial  $\text{SO}_4^{2-}$  concentrations ( $R^2=0.97$ ;  $R^2=0.92$ ). The increasing  
31 abundance of sulfate reduction bacteria (SRB) was also linearly correlated with initial  
32  $\text{SO}_4^{2-}$  concentrations ( $R^2=0.96$ ), ranging from  $6.65 \times 10^7$  to  $1.97 \times 10^8$  copies/g. However,  
33 the  $\text{Fe}^{2+}$  concentrations displayed a negative correlation with initial  $\text{SO}_4^{2-}$   
34 concentrations, and the final  $\text{Fe}^{2+}$  concentrations were 9.68, 7.07, 6.5, 5.57, 4.42 and  
35 3.46 mg/L, respectively. As a result, the released TP in the overlying water, to promote  
36 the eutrophication, was up to 1.4 mg/L in the treatment of 150 mg/L  $\text{SO}_4^{2-}$  concentration.  
37 Therefore, it is necessary to consider the effect of rapidly increasing  $\text{SO}_4^{2-}$   
38 concentrations on the release of endogenous phosphorus and the eutrophication in lakes.

### 39 **1.Introduction**

40 Nowadays, cyanobacteria bloom in eutrophic lakes has become one of the most  
41 serious problems in freshwater lakes all over the world (Iwayama et al., 2017; Ho et al.,  
42 2019). Phosphorus, as a necessary nutrient for biological growth, is considered to be  
43 one of the main limiting factors of lake eutrophication (Ni et al., 2020). In recent years,  
44 the input of exogenous phosphorus has been effectively controlled, while the release of

45 endogenous phosphorus is still an urgent problem in eutrophic lakes (Liu et al., 2018;  
46 Guo et al., 2020). The release of endogenous phosphorus is affected by many factors,  
47 such as wind and wave and the cyanobacteria decomposition (Xu et al., 2018; Zhao et  
48 al., 2019). There are many forms of phosphorus in freshwater lake sediments, including  
49 aluminum bound phosphorus (Al-P), iron bound phosphorus (Fe-P), etc. Among them,  
50 Fe-P, formed under the condition of high dissolved oxygen (DO), is the most active  
51 form of phosphorus in the sediments, which has a more obvious response to the change  
52 of DO (Zhang et al., 2020). The accumulation and decay of cyanobacteria in eutrophic  
53 lakes will change the physical and chemical environments of water body and form  
54 anaerobic reduction conditions (Yan et al., 2017). This will facilitate the reduction of  
55 iron oxides and lead to the desorption and release of Fe-P in sediments, resulting in the  
56 increase of endogenous phosphorus release (Zhao et al., 2019).

57 Iron reduction plays an important role in natural ecosystems. It has been reported  
58 that dissimilatory reduction of iron accounts for 22% of the total amount of organic  
59 matter anaerobic mineralization in offshore areas (Thamdrup et al., 2004). According  
60 to the classical theory, iron oxides or hydroxides can adsorb phosphorus in the water  
61 and form Fe-P precipitation (Gunnars et al., 1997). In freshwater lakes, the lack of Fe(III)  
62 content or the diagenesis of organic phosphorus may be the reason for the lack of  
63 phosphorus in the overlying water. Therefore, the formation of iron oxides on the  
64 surface of sediments is closely related to the phosphorus cycle process (Amirbahman  
65 et al., 2003; Chen et al., 2014). The interaction between iron and phosphorus is reflected  
66 in the effect of adsorption and desorption of Fe oxide on the P content in the overlying

67 water, since Fe-P is the main internal source of phosphorus (Wu et al., 2019). Iron  
68 oxides can be used as both the source and destination of phosphorus in lake ecosystems  
69 (Mort et al., 2010; Azam et al., 2014). In anaerobic reduction environments, iron  
70 reduction can significantly promote the resolution of Fe-P. The  $\text{Fe}^{2+}$  generated by the  
71 reaction can form FeS solid with soluble sulfide. In addition, free  $\text{Fe}^{3+}$  will combine  
72 with humus to form stable complex, which further prevents the co-precipitation process  
73 of phosphorus and iron oxides (Mort et al., 2010; Zhang et al., 2020). Therefore, iron  
74 reduction process driven by cyanobacteria decomposition affects the circulation of  
75 phosphorus in freshwater lakes.

76 Due to the  $\text{SO}_4^{2-}$  concentration in seawater reaching 28 mM, sulfate reduction  
77 process with the participation of sulfate reduction bacteria (SRB) has received  
78 considerable attention in the basic material cycle of marine biogeochemistry (Fike et  
79 al., 2015; Pan et al., 2020). In freshwater lakes, the  $\text{SO}_4^{2-}$  concentration is less than 800  
80  $\mu\text{M}$ , which is generally considered insufficient for continuous sulfate reduction (Hansel  
81 et al., 2015). However, in recent years, with the continuous input of exogenous sulfur,  
82 the  $\text{SO}_4^{2-}$  concentration in freshwater lakes increases significantly and the degree of the  
83 eutrophication and the  $\text{SO}_4^{2-}$  concentration show a positive correlation (Dierberg et al.,  
84 2011; Yu et al., 2013). For instance, the  $\text{SO}_4^{2-}$  concentration in Lake Taihu, one of the  
85 typical eutrophic lakes worldwide, has increased from 30 to 100 mg/L in the past 70  
86 years and it will continue to rise in the future (Yu et al., 2013; Zhou et al., 2022). The  
87 impact of sulfate reduction on the material cycle of lake ecosystems may be far beyond  
88 our knowledge (Baldwin et al., 2012; Yu et al., 2013). On the other hand, it has been

89 reported that sulfate reduction process is one of the important ways of anaerobic  
90 metabolism of organic matter in freshwater lakes, and  $\sum S^{2-}$  produced by sulfate  
91 reduction process can mediate the iron reduction process (Jorgensen et al., 2019; Zhang  
92 et al., 2020). SRB mainly uses  $SO_4^{2-}$  as the electron acceptor to complete anaerobic  
93 respiration, and the sulfur compounds produced by anaerobic metabolism are bound  
94 with iron and so on, which are fixed in the sediments and form AVS on the surface of  
95 sediments (Holmer et al., 2001; Chen et al., 2016). Therefore, with the input of  
96 exogenous sulfur, sulfate reduction process produced  $\sum S^{2-}$  will further promote iron  
97 reduction in freshwater lakes.

98 In freshwater lakes, iron cycle affects the process of phosphorus cycle, and sulfur  
99 cycle plays an important role in regulating iron cycle. Therefore, the cycle of iron, sulfur  
100 and phosphorus in freshwater lakes is inseparable (Wu et al., 2019; Zhao et al., 2019).  
101 Studies have shown that even when  $SO_4^{2-}$  content was as low as 20 mg/L, the anaerobic  
102 metabolism of organic substrates was still dominated by sulfate reduction. Therefore,  
103 sulfate reduction process plays an important role in the lacustrine biochemical cycle  
104 (Hansel et al., 2015). In the absence of cyanobacteria, sulfate reduction doesn't occur  
105 even if the  $SO_4^{2-}$  concentration is higher (Zhao et al., 2021). This is because the  
106 accumulation and decomposition of cyanobacteria not only change the environment of  
107 water body, but also release a large amount of organic matter, which provides the  
108 necessary conditions for the circulation of iron, sulfur and phosphorus (Yan et al., 2017;  
109 Melemdez-Pastor et al., 2019). Therefore, under the co-effect of the increase of  $SO_4^{2-}$   
110 and the cyanobacteria decomposition, the sulfate reduction process and the effect of

111 iron reduction process on endogenous phosphorus release from sediments need to be  
112 further studied.

113 In this study, a series of different initial concentrations of  $\text{SO}_4^{2-}$  were set according  
114 to the variation trend of  $\text{SO}_4^{2-}$  concentrations over the years and the possible rising trend  
115 of eutrophic Lake Taihu. The effects of increased  $\text{SO}_4^{2-}$  concentration and cyanobacteria  
116 bloom on sulfate reduction coupled with the microbial processes were investigated. The  
117 dynamic changes of  $\text{Fe}^{2+}$  and  $\text{Fe}^{3+}$  concentrations during iron reduction were studied in  
118 order to reveal the effect of sulfate reduction on iron reduction. In addition, the dynamic  
119 changes of phosphorus in the overlying water and sediment were investigated. Finally,  
120 the coupled sulfate, iron and phosphorus cyclic processes affected by the increasing  
121 sulfate concentration and cyanobacteria bloom were also comprehensively analyzed for  
122 elucidating the phosphorus release dynamics to tracking the hidden promoter of  
123 cyanobacteria bloom in eutrophic lakes. The findings may be benefit for evaluating the  
124 effect of sulfate reduction in freshwater lakes and its impact on the promotion of iron  
125 reduction and the release of endogenous phosphorus.

## 126 **2. Materials and methods**

### 127 *2.1 Sample collection and preparation*

128 Lake Taihu ( $31^{\circ}24'40''\text{N}$ ,  $120^{\circ}1'3''\text{E}$ ), one of the largest eutrophic shallow lakes  
129 in China, with an average depth of 2.4 m and an area of 2340  $\text{m}^2$  (Mao et al., 2021). In  
130 this study, samples of sediments and cyanobacteria were collected in July 2020.  
131 Sediments (0-20 cm) from the west shoreline of the lake ( $31^{\circ}24'45''\text{N}$ ,  $120^{\circ}0'42''\text{E}$ )  
132 were collected using a gravity core sampler (length of 150 cm and diameter of 20 cm).

133 Cyanobacteria was collected and concentrated by sieving water through a fine-mesh  
134 plankton (250 mesh). All the sediment and cyanobacteria samples were stored in an  
135 incubator with ice packs and delivered to the laboratory immediately. The sediment  
136 samples were blended thoroughly, homogenized, and sieved (100 mesh) to the  
137 polyethylene bag. The cyanobacteria samples were flushed and centrifuged at 1500  
138 r/min for 5 min by a CT15RT versatile refrigerated centrifuge (China) and freeze  
139 drying by Biosafer-10A. Different gradient sulfate concentrations were prepared from  
140 the high purity water and Na<sub>2</sub>SO<sub>4</sub>.

#### 141 *2.2 Set-up of incubation microcosms*

142 To simulate the dramatical SO<sub>4</sub><sup>2-</sup> increase and cyanobacteria blooms of eutrophic  
143 Lake Taihu, a series of microcosms were constructed in this study. According to the  
144 ratio of surface sediments and the average water depth and the cyanobacteria  
145 accumulation density of 2500 g/m<sup>2</sup> during the breakout of cyanobacteria blooms of  
146 Taihu Lake, 100 g of sediment, 200 ml of water and 0.11 g of cyanobacteria powder  
147 were added into each bottle (Zhang et al., 2020). Meanwhile, according to the change  
148 trend of SO<sub>4</sub><sup>2-</sup> concentrations in Taihu Lake over the years and the possibility of further  
149 increase in the future (Yu et al., 2013), the SO<sub>4</sub><sup>2-</sup> concentrations in six microcosm  
150 systems were configured as: 30, 60, 90, 120, 150 mg/L, and a control without SO<sub>4</sub><sup>2-</sup>,  
151 respectively. The microcosm system adopted anaerobic bottles ( $\Phi$ 75 mm, length 180  
152 mm, volume 500 ml) as the reaction device. There were three replicates in each SO<sub>4</sub><sup>2-</sup>  
153 concentration experimental group. Each group was sampled 17 times on 1, 2, 3, 4, 5, 6,  
154 7, 9, 11, 14, 18, 23, 28, 33, 38, 43 and 48 d. Totally, there were 306 anaerobic bottles,

155 and all the anaerobic bottles were placed in a biochemical incubator at a temperature of  
156 25 °C. The water, gas and soil samples were collected by destructive sampling, that is,  
157 at each sampling point, 18 anaerobic bottles were opened for testing, which ensured the  
158 anaerobic environment and air pressure for other bottles. A part of sediment was used  
159 for microbe determination and kept in a refrigerator at -80 °C, and the rest sediment and  
160 other samples were kept at 0-4 °C for less than 24 h before analysis.

### 161 *2.3 Chemical analytical methods*

162 All water samples were filtered through 0.45µm Nylon filters. Dissolved total  
163 phosphorus (DTP) was determined by colorimetry after digestion with  $K_2S_2O_8+NaOH$ ,  
164 and the ammonium molybdate and ascorbic acid were used as chromogenic agents  
165 (Ebina et al., 1983). Water DO, oxidation and reduction potential (ORP) were measured  
166 using calibrated probes (MP525, China) during destructive sampling. The  $SO_4^{2-}$  was  
167 detected using the turbidimetric method with the stabilizer of  $BaCl_2$  and gelatin  
168 (Tabatabai et al., 1974), and the  $\sum S^{2-}$  was detected by methylene blue (Cline et al.,  
169 1969).  $Fe^{2+}$  and  $Fe^{3+}$  was determined by colorimetric (Phillips et al., 1987). The  
170 sediment total phosphorus (TP) was extracted and determined by colorimetry (Ruban  
171 et al., 2001). The schematic diagram of the method to test acid volatile sulfate (AVS)  
172 was showed in Fig.S5, briefly, 5 g sediment was put into a 250 ml glass flask and inside  
173 a small beaker with 15 ml of  $ZnAc_2 \cdot 2H_2O$  and  $NaAc \cdot 3H_2O$  was used to absorb  $H_2S$  gas.  
174 The tube A was connected by  $N_2$  and continue for 5 minutes, then closed valve. 2 ml  
175 ascorbic acid solution was added to prevent  $S^{2-}$  oxidation, and then 15 ml (6 mol/L)  
176 hydrochloric acid was added with the reaction at room temperature for 18 h. AVS was



177 determined by zinc cold diffusion method (Hsieh et al., 1997).

#### 178 *2.4 Quantification of SRB in sediments*

179 In order to confirm the changes of sediment SRB in the microcosms, RT-QPCR  
180 technologies were used to determine the cell copy numbers of MPA and SRB on 0,7  
181 and 38 d in the sediments.

182 The sediment samples were collected and frozen at -80 °C in an ultra-low  
183 temperature freezer. The E.Z.N.A. ®Soil DNA Kit (Omega Bio-Tek, Norcross, GA,  
184 USA) was used to extract the total genomic DNA from each soil sample according to  
185 the manufacturer's instructions. Nucleic acid quality and concentration were  
186 determined by 1% agarose gel electrophoresis and NanoDrop 2000 UV  
187 spectrophotometer (Thermo Scientific, USA), respectively.

188 SRB in sediments were quantified using the quantitative polymerase chain  
189 reaction (qPCR) method. The qPCR with primer sets targeting DSR1F+ (5'-  
190 ACSCACTGGAAGCACGGCGG-3') and DSR-R (5'-GTGGMRCCGTGCAKRTT  
191 GG-3') were used for the SRB in this study. The q-PCR experiments were performed  
192 on a ABI7300 q-PCR instrument (Applied Biosystems, USA) using ChamQ SYBR  
193 Color qPCR Master Mix as the signal dye. Each 20 µL reaction mixture contained 2 µL  
194 of the template DNA and 16.5 µL of ChamQ SYBR Color qPCR Master Mix. Standard  
195 curves for each gene were obtained by the tenfold serial dilution of standard plasmids  
196 containing the target functional gene. All operations were followed the MIQE  
197 guidelines.

#### 198 *2.5 Statistical analysis*

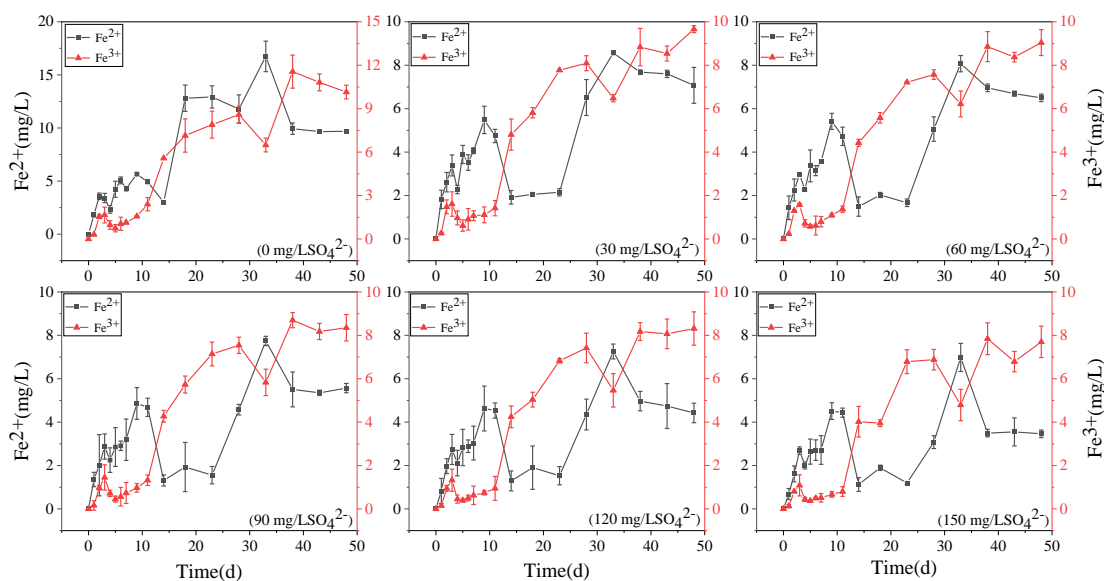
199 The Statistical Package of the Social Science 18.0 (SPSS 18.0) was used for  
200 statistical analysis. The one-way analysis of variance (ANOVA) and correlation  
201 analysis was carried out using bivariate correlations analysis.

202

### 203 **3.Results**

#### 204 *3.1 Fe<sup>2+</sup> and Fe<sup>3+</sup> dynamics in overlying water*

205 The concentration variations of Fe<sup>2+</sup> and Fe<sup>3+</sup> in overlying water during the  
206 incubation was presented in Fig.1. In the treatment without SO<sub>4</sub><sup>2-</sup>, they increased  
207 continuously to 9.68 mg/L and 10.15 mg/L, respectively. The concentration of Fe<sup>3+</sup> in  
208 the remaining five treatments decreased at the beginning and then increased to keep  
209 stable. The higher the initial sulfate concentration was, the lower the final Fe<sup>3+</sup>  
210 concentration displayed. In the initial 150 mg/L SO<sub>4</sub><sup>2-</sup> concentration treatment, the final  
211 Fe<sup>3+</sup> concentration was the lowest of 7.7 mg/L. The Fe<sup>2+</sup> concentration in the five  
212 treatments supplemented with SO<sub>4</sub><sup>2-</sup> decreased significantly from 11 d to 23 d, and then  
213 increased to a stable level. The final concentration of Fe<sup>2+</sup> also showed a negative  
214 correlation with the initial concentration of SO<sub>4</sub><sup>2-</sup>. In the initial 30 mg/L SO<sub>4</sub><sup>2-</sup>  
215 concentration treatment, the final Fe<sup>2+</sup> concentration was the highest of 7.07 mg/L.



216

217 Figure 1. The concentration variations of  $\text{Fe}^{2+}$  and  $\text{Fe}^{3+}$  in the water column during the  
 218 incubation

219 *3.2  $\text{SO}_4^{2-}$  and  $\sum\text{S}^{2-}$  dynamics in overlying water*

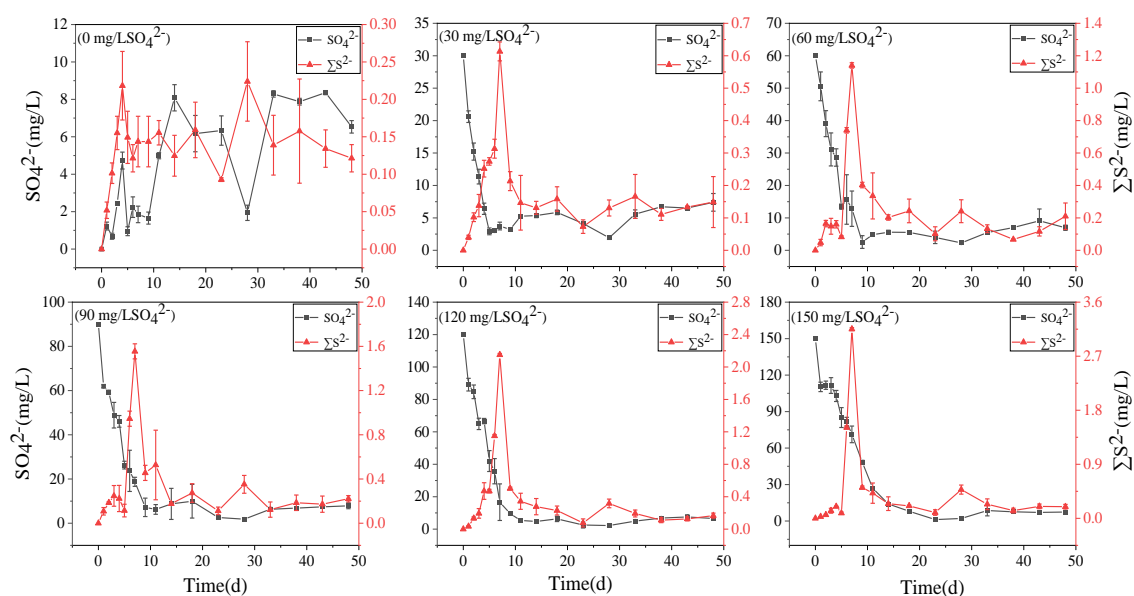
220 All treatments had obvious sulfate reduction reaction, and the concentration of  
 221  $\text{SO}_4^{2-}$  decreased greatly except for the treatment without adding  $\text{SO}_4^{2-}$  (Fig.2). The  
 222 higher the initial sulfate concentration was, the faster the sulfate reduction rate in the  
 223 initial stage exhibited (Tab.1). In the treatment with initial  $\text{SO}_4^{2-}$  concentration of 150  
 224 mg/L, the sulphate reduction rate was 39.68 mg/L·d, while it was only 9.39 mg/L·d in  
 225 the 30 mg/L  $\text{SO}_4^{2-}$  treatment. The sulfate reduction rate at the beginning of other  
 226 treatments was also positively correlated with the initial  $\text{SO}_4^{2-}$  concentration.

227 The higher the initial  $\text{SO}_4^{2-}$  concentration was, the higher the maximum  
 228 concentration of  $\sum\text{S}^{2-}$  was. In the treatment with initial  $\text{SO}_4^{2-}$  concentration of 30 mg/L,  
 229 the lowest concentration was 2.93 mg/L on the 5th day. However, the lowest  $\text{SO}_4^{2-}$   
 230 concentration appeared on the 23rd day was 1.18 mg/L in the treatment with initial  
 231  $\text{SO}_4^{2-}$  concentration of 150 mg/L. The maximum concentration of  $\sum\text{S}^{2-}$  was positively

232 correlated with the initial  $\text{SO}_4^{2-}$  concentration. In the initial  $\text{SO}_4^{2-}$  concentrations of 30,  
 233 60, 90, 120 and 150 mg/L  $\text{SO}_4^{2-}$  treatments, the highest  $\Sigma\text{S}^{2-}$  concentrations at 7 d were  
 234 0.14, 0.61, 1.14, 1.55, 2.15, and 3.15 mg/L, respectively.

235 Table 1. Sulphate reduction rate in the water column of microcosms (mg/L·d)

| $\text{SO}_4^{2-}$ (mg/L) \ Time(d) | 0     | 7     | 38   |
|-------------------------------------|-------|-------|------|
| 0                                   | -     | -     | -    |
| 30                                  | 9.39  | 0.74  | 0.05 |
| 60                                  | 9.44  | 2.84  | 0.07 |
| 90                                  | 28.02 | 4.98  | 0.11 |
| 120                                 | 30.89 | 19.45 | 0.11 |
| 150                                 | 39.68 | 10.42 | 0.21 |



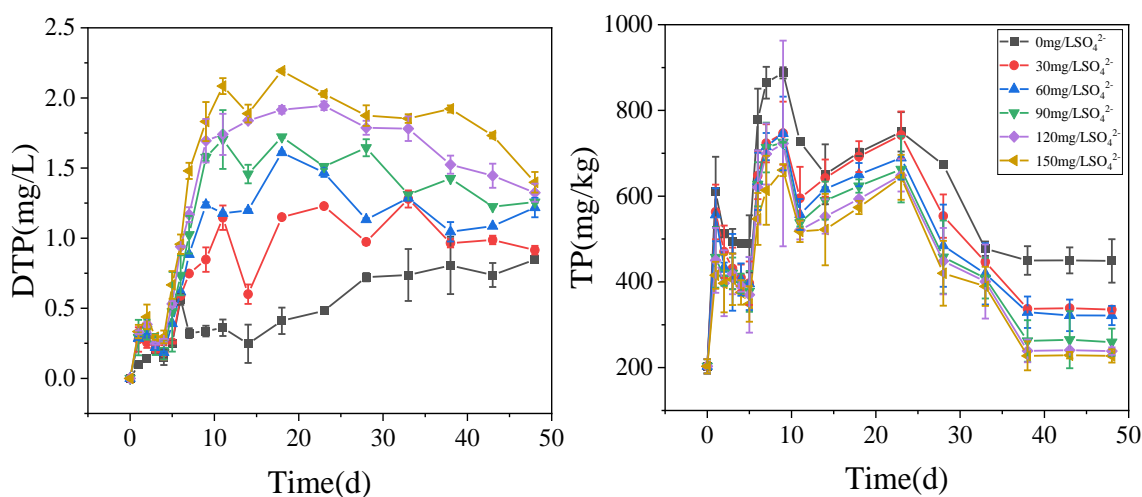
236  
 237 Figure 2. The concentration variations of  $\text{SO}_4^{2-}$  and  $\Sigma\text{S}^{2-}$  in the water column during the  
 238 incubation

### 239 3.3 TP dynamics in overlying water and sediments

240 The dynamics of DTP concentrations in overlying water during the incubation was  
 241 presented (Fig.3 left). The concentrations of DTP in overlying water were positively  
 242 correlated with the initial  $\text{SO}_4^{2-}$ . The higher the initial concentrations of  $\text{SO}_4^{2-}$  were, the

243 higher the concentrations of DTP in overlying water were. On 11 day, DTP in overlying  
 244 water continued to rise and then kept stable. The highest DTP concentration was 2.08  
 245 mg/L in the treatment with initial  $\text{SO}_4^{2-}$  concentration of 150 mg/L, while the highest  
 246 DTP concentration was 0.36 mg/L in the treatment without  $\text{SO}_4^{2-}$  addition.

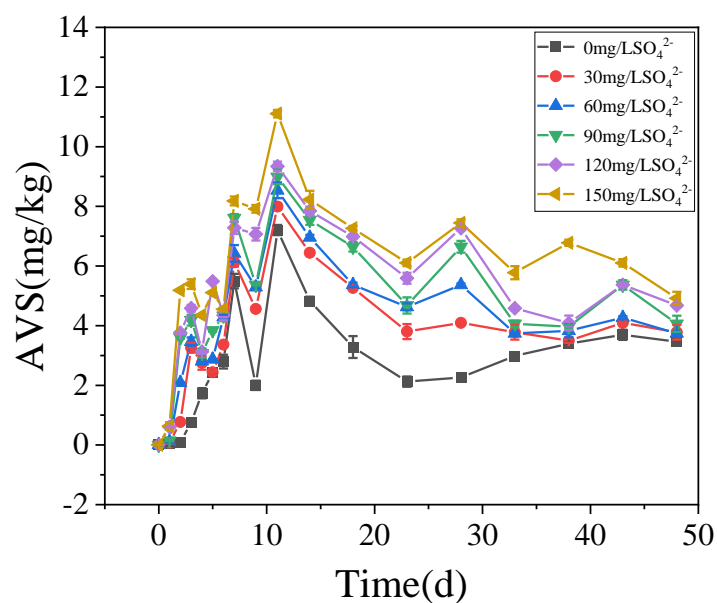
247 The concentrations of TP in the sediments increased significantly in all treatments  
 248 with the cyanobacteria decomposition in the initial stage (Fig.3 right). Among of all  
 249 treatments, on 9<sup>th</sup> day, the highest concentration of TP in the sediments was 887.69  
 250 mg/kg in the treatment with initial  $\text{SO}_4^{2-}$  concentration of 0 mg/L. After 23 days, TP in  
 251 the sediments decreased significantly and then stabilized. During cyanobacteria  
 252 decomposition and sulfate reduction, the concentrations of TP in all treatments  
 253 negatively correlated with the initial  $\text{SO}_4^{2-}$  concentration. The final TP concentration  
 254 was 448.92, 335.32, 321.56, 259.32, 238.56 and 227.21 mg/kg, respectively in all  
 255 treatments.



256  
 257 Figure 3. The concentrations of TP in the overlying water (left) and sediments (right)  
 258 during the incubation

259 *3.4 AVS dynamics in the sediments*

260 The concentrations of AVS in the sediments were positively correlated with the  
 261 initial  $\text{SO}_4^{2-}$  concentrations. With the increase of TP in overlying water, the AVS in the  
 262 sediments also increased steadily and reached the peak on the 11st days. In the treatment  
 263 with initial  $\text{SO}_4^{2-}$  concentration of 0, 30, 60, 90, 120 and 150 mg/L, the highest  
 264 concentration of AVS in the sediments were 7.21, 7.99, 8.54, 8.99, 9.34 and 11.11  
 265 mg/kg, respectively.



266  
 267 Figure 4. The concentration of AVS in the sediments during the incubation

### 268 3.5 SRB dynamics in the sediments

269 During the decomposition of cyanobacteria, the SRB abundance significantly  
 270 increased compared with the initial stage ( $P < 0.01$ ). In the initial stage, the SRB  
 271 abundance was  $1.09 \times 10^8$  copies/g and the final value was positively correlated with the  
 272 initial  $\text{SO}_4^{2-}$ . On 7 d, SRB of all treatments showed a downward trend compared with  
 273 the initial value, and there was no significant difference in SRB values between each  
 274 treatment. On 38 d, except for the initial  $\text{SO}_4^{2-}$  concentrations of 0 and 30 mg/L, SRB  
 275 increased significantly in other treatments.

276 Table 2. Copy numbers of the *dsrB* gene of SRB in the sediments during the incubation  
 277 (copies/g)

| Time<br>SO <sub>4</sub> <sup>2-</sup> (mg/L) | 0 d                  | 7 d                  | 38 d                 |
|--|----------------------|----------------------|----------------------|
| 0  | 1.09×10 <sup>8</sup> | 5.81×10 <sup>7</sup> | 6.65×10 <sup>7</sup> |
| 30   | 1.09×10 <sup>8</sup> | 6.13×10 <sup>7</sup> | 7.71×10 <sup>7</sup> |
| 60   | 1.09×10 <sup>8</sup> | 7.61×10 <sup>7</sup> | 1.15×10 <sup>8</sup> |
| 90   | 1.09×10 <sup>8</sup> | 7.87×10 <sup>7</sup> | 1.31×10 <sup>8</sup> |
| 120  | 1.09×10 <sup>8</sup> | 7.99×10 <sup>7</sup> | 1.49×10 <sup>8</sup> |
| 150  | 1.09×10 <sup>8</sup> | 8.23×10 <sup>7</sup> | 1.91×10 <sup>8</sup> |

278 **4. Discussion**

279 It is generally acknowledged that climate warming and exogenous nutrient input  
 280 are the important contributors to the occurrence of cyanobacteria blooms (Anneville et  
 281 al., 2015; Yan et al., 2017). However, in this study, we found that the dramatically  
 282 increasing SO<sub>4</sub><sup>2-</sup> concentration in eutrophic lakes is also a non-negligible promoter for  
 283 the self-sustaining of cyanobacteria blooms. In eutrophic lakes, the decomposition of  
 284 cyanobacteria consumed DO in the water, and formed strong anaerobic reduction  
 285 conditions (Fig.S1). Fe-P was desorbed to from free Fe<sup>3+</sup>, which was reduced to Fe<sup>2+</sup> in  
 286 anaerobic environments (Fig.1). Free Fe<sup>2+</sup> combined with ΣS<sup>2-</sup> which generated by  
 287 sulfate reduction and eventually formed AVS fixed in the sediments (Fig.4), and  
 288 phosphorus was released from the sediments (Fig.3). It has been reported that SRB and  
 289 iron reduction bacteria (IRB) are the main microorganisms that drive sulfate reduction  
 290 and iron reduction, respectively, and cyanobacteria decomposition promotes these  
 291 microorganisms' growth (Wu et al., 2018). Consistent with these results, our findings  
 292 also revealed that cyanobacteria released large amounts of organic matter to promote  
 293 microbial growth during their decay and decomposition (Fig.S2, Tab. 2) and ultimately

294 promoted anaerobic reduction of sulfur and iron (Holmer et al., 2001). Therefore, with  
295 increasing  $\text{SO}_4^{2-}$  concentrations in eutrophic lakes, the influence of sulfate reduction on  
296 phosphorus release is worth further investigation.

297 Sulfur and iron in eutrophic lake sediments are directly related to iron and  
298 phosphorus, and sulfur and phosphorus are also closely linked to bridges under the  
299 action of iron (Zhang et al., 2020). With the increase of  $\text{SO}_4^{2-}$  concentration in eutrophic  
300 lakes, the effect of sulfate reduction on phosphorus release from sediments may be more  
301 important than previously recognized (Pester et al., 2012). Sulfate reduction driven by  
302 SRB is an important organic metabolism pathway in natural systems. During the sulfate  
303 reduction process,  $\text{SO}_4^{2-}$  is an electron acceptor and its concentration variation can  
304 significantly affect the sulfate reduction rate (Holmer et al., 2001; Nakagawa et al.,  
305 2012).  $\text{SO}_4^{2-}$  is reduced to  $\sum\text{S}^{2-}$  by acquiring the electrons supplied by SRB oxidation,  
306 and thus SRB plays an important role in sulfate reduction (Sela-Adler et al., 2017). The  
307 increase of  $\text{SO}_4^{2-}$  concentration promotes the SRB abundance, as evidenced by a  
308 positive correlation (Wu et al., 2018). In the case of increased SRB abundance (Tab. 2)  
309 and increased  $\text{SO}_4^{2-}$  concentration, the sulfate reduction reaction was enhanced. The  
310  $\text{SO}_4^{2-}$  concentration in the overlying water decreased significantly accompanied by a  
311 temporary increase in  $\sum\text{S}^{2-}$  (Fig.2). The highest concentrations of  $\sum\text{S}^{2-}$  also increased  
312 with the initial  $\text{SO}_4^{2-}$  concentrations (Fig.5a). Interestingly, the  $\sum\text{S}^{2-}$  decreased rapidly  
313 after day 10 to almost zero at the end (Fig.2). This may result from the two keys: (a)  
314 hydrogen sulfide overflows from the incubator; (b) sulfide migrates downward, and  
315 combines with other substances in the sediment and is immobilized (Zhang et al., 2020).



316 In this study, TP in the overlying water has a significant positive correlation with the  
317 initial  $\text{SO}_4^{2-}$  concentrations ( $R^2 = 0.96$ ; Fig.3). The classical theory presumes that iron  
318 reduction by IRB leads to the release of iron-bound phosphorus in the anaerobic layer  
319 of sediments, and when the formed  $\text{Fe}^{2+}$  enters the aerobic water layer, it is oxidized by  
320  $\text{Fe}^{3+}$  and bound to phosphorus again (Roden et al., 2006; Chen et al., 2016). When the  
321 sulfate reduction process mediates the iron reduction process, the released  $\text{Fe}^{2+}$   
322 combines with the product  $\sum\text{S}^{2-}$  of sulfate reduction to form Fe-S, thus weakening the  
323 reoxidation process of  $\text{Fe}^{2+}$ , and increasing the release of phosphorus (Mort et al., 2010;  
324 Zhao et al., 2019). Therefore, with the increase of  $\text{SO}_4^{2-}$  concentrations in eutrophic  
325 lakes, it significantly promoted the release of endogenous phosphorus from the  
326 sediments.

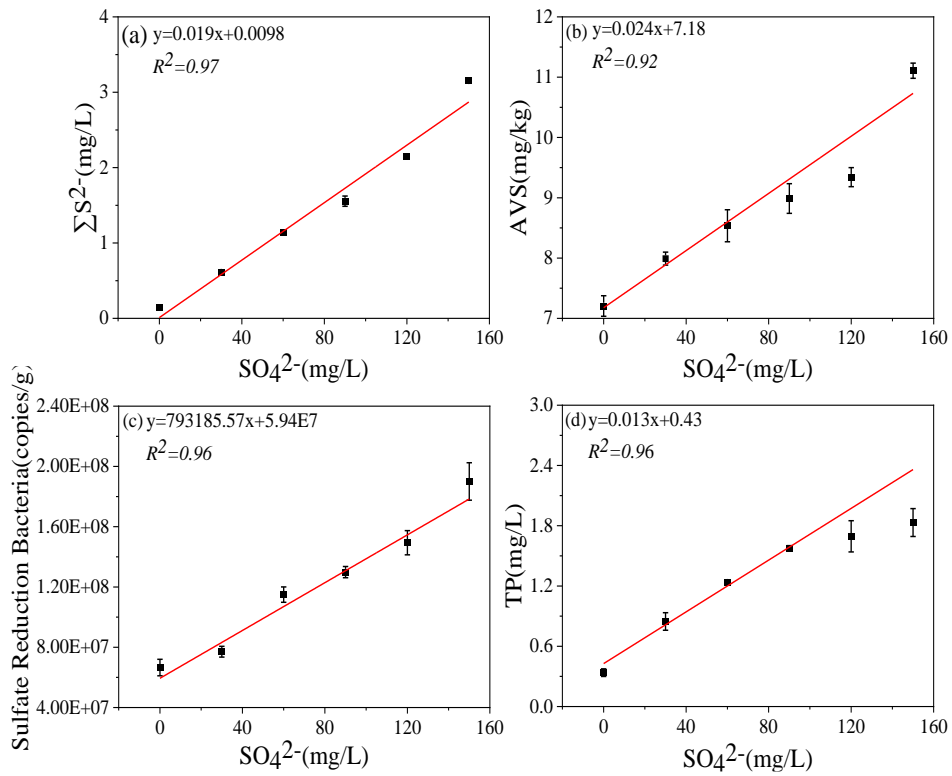
327 Although from a thermodynamic point of view, iron reduction should take  
328 precedence over sulfur reduction (Han et al., 2015). However, due to chemical kinetics,  
329 sulfur reduction occurs before iron reduction, resulting in the simultaneous appearance  
330 of  $\sum\text{S}^{2-}$  and iron oxides (Han et al., 2015; Hansel et al., 2015). This is consistent with  
331 the concentration variation of iron and sulfur in this study (Fig.1-3). It has been reported  
332 that iron cycles in the water body will produce an intense response to the accumulation  
333 of sulfide, that is, sulfate reduction can promote iron reduction (Friedrich et al., 2014;  
334 Zhang et al., 2020).  $\sum\text{S}^{2-}$  is the final product of sulfate reduction, which is toxic to  
335 microorganisms and easy to combine with heavy metals such as  $\text{Fe}^{2+}$  to form AVS in  
336 lake sediments (Holmer et al., 2001). In this study, the concentration of AVS showed a  
337 significant positive correlation with the initial concentration of  $\text{SO}_4^{2-}$  (Fig. 4, 5b), which

338 was consistent with the highest concentration of  $\sum S^{2-}$  observed in the overlying water  
339 (Fig. 2, 5c). The concentrations of  $Fe^{2+}$  and  $Fe^{3+}$  in the overlying water increased  
340 significantly, and  $Fe^{2+}$  significantly decreased in the middle of the incubation (Fig. 1),  
341 suggesting that  $Fe^{2+}$  reduced by sulfate can be combined with the product  $\sum S^{2-}$  (Fig. 2).  
342 These results consistent with the trend that AVS in the sediments reached a peak after  
343 11 days and  $\sum S^{2-}$  in the water decreased rapidly after 9 days and remained at a lower  
344 concentration (Fig. 2, 3). The reason for this phenomenon may be the formation of Fe-  
345 S compounds that is finally fixed in the sediments (Zhao et al., 2019).

346 The  $\sum S^{2-}$  mediated iron chemical reduction may lead to more environmental  
347 effects, such as phosphorus mobilization (Zhang et al., 2020). For instance, a previous  
348 investigation on the lakes along the Yangtze River demonstrates that the effects of  
349 endogenous phosphorus release is probably related to the increase of  $SO_4^{2-}$   
350 concentration (Chen et al., 2016). In this study, the concentration of  $Fe^{2+}$  in the  
351 treatment without  $SO_4^{2-}$  continued to rise, and was up to the highest concentration  
352 among all treatments (Fig. 1). In contrast, the concentrations of TP in the treatment  
353 without  $SO_4^{2-}$  showed the lowest concentration among all treatments (Fig. 1, 5a). This  
354 is caused by  $Fe^{2+}$  and  $Fe^{3+}$  recombining with phosphorus and being immobilized in the  
355 sediments (Wu et al., 2019). In general, iron combines with phosphorus to form siderite  
356 ( $FePO_4 \cdot 2H_2O$ ) and blue iron ( $Fe_3(PO_4)_2 \cdot 8H_2O$ ) and is bound to the sediments (Taylor  
357 et al., 2011). However, when precipitation or reduction separates iron from iron  
358 phosphate minerals, phosphorus bound to iron is released (Gu et al., 2016).

359 In order to further elucidate whether the increasing  $SO_4^{2-}$  concentrations in

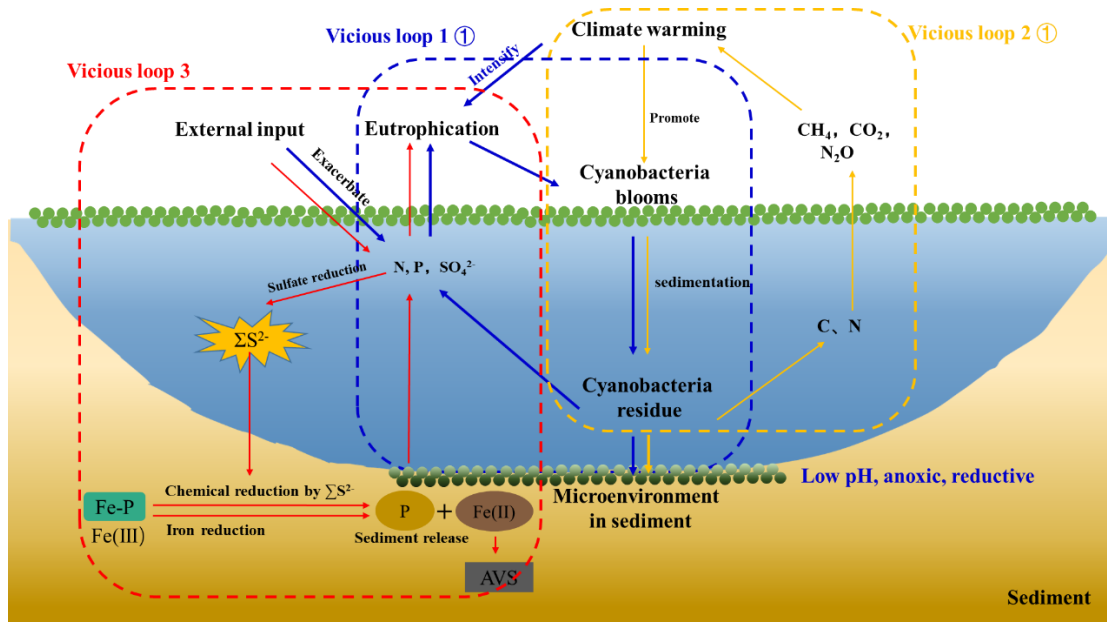
360 overlying water result in the self-sustaining of eutrophication in shallow lakes, a  
361 conceptual diagram was put forward (Fig. 6). It has been accepted that exogenous  
362 nutrient inputs and climate warming have positive effects on the breakout of  
363 cyanobacteria blooms. With the continuous input of exogenous sulfur, the  $\text{SO}_4^{2-}$   
364 concentration in the lake water increases significantly. When cyanobacteria blooms  
365 start to decay, the overlying water shifts from the aerobic state to the strong anaerobic  
366 state, providing carbon source to promote the growth of microorganisms such as SRB.  
367 The increasing  $\text{SO}_4^{2-}$  concentrations provide the electron for the sulfate reduction  
368 process, resulting in the sulfate reduction and the release of a large amount of  $\sum\text{S}^{2-}$ . The  
369  $\text{Fe}^{2+}$  released from the iron reduction process is captured by  $\sum\text{S}^{2-}$ , and finally the  
370 combination of iron and P was reduced, promoting the release of endogenous  
371 phosphorus. Therefore, it is necessary to pay attention to the effect of enhanced sulfate  
372 reduction on endogenous phosphorus release in eutrophic lakes.



373

374 Figure 5. Correlation of initial  $\text{SO}_4^{2-}$  concentrations with  $\Sigma\text{S}^{2-}$  (a), AVS(b), Sulfate-  
 375 reducing bacteria (SRB) (c), TP (d) in the microcosm systems, respectively.

376



377

378 Figure 6. A simplified scheme of the relationship among climate warming, lake  
 379 eutrophication and cyanobacteria blooms in eutrophic lakes. Under climate warming

380 scenarios, extreme abiotic and biotic conditions facilitated the breakout of  
381 cyanobacteria blooms. After their collapse, the high amount of N, P, and C were  
382 released into the overlying water and reacted with the eutrophication. Furthermore, a  
383 large amount of CH<sub>4</sub> and CO<sub>2</sub> was produced and emitted to the atmosphere, contributing  
384 to global warming of freshwater lakes (Yan et al. 2017). With the external sulfur input,  
385 the concentration of SO<sub>4</sub><sup>2-</sup> increased significantly and sulfate reduction was enhanced.  
386 The cyanobacteria decomposition created an anaerobic reduction environment, which  
387 will promote iron reduction and sulfate reduction. The free Fe<sup>3+</sup> generated by Fe-P  
388 desorption was reduced to Fe<sup>2+</sup> and combined with ΣS<sup>2-</sup> which produced by sulfate  
389 reduction to form stable Fe-S in the sediments. Phosphorus was released from the  
390 sediment into the overlying water. Therefore, there are three vicious loops between  
391 cyanobacteria blooms occurrence, lake eutrophication and climate warming.

392

## 393 **5. Conclusion**

394 The dramatical increase of SO<sub>4</sub><sup>2-</sup> concentration was up to more than 100 mg/L in  
395 eutrophic lakes. There was a coupling relationship between sulfur, iron and phosphorus  
396 cycles in lake ecosystems. Rapidly increasing sulfate concentration enhanced the  
397 sulfate reduction to release of a large amount of ΣS<sup>2-</sup> mediated by the increasing  
398 abundance of SRB with the adequate organic source from the decay processes of  
399 cyanobacteria blooms. The iron reduction, in positive with initial sulfate concentration,  
400 occurred with the cyanobacteria decomposition. The Fe<sup>2+</sup> released from the iron  
401 reduction process was captured by ΣS<sup>2-</sup>, and finally the combination of iron and P was

402 reduced, promoting the release of endogenous phosphorus. Therefore, except for  
403 climate warming and excessive nutrients, the increasing sulfate concentration is proved  
404 to be another hidden promoter of eutrophication in shallow lakes.

405

#### 406 **Author contributions**

407 Xu Xiaoguang: designed and led the study. Zhou Chuanqiao, Peng Yu, Chen Li,  
408 Yu Miaotong, Muchun Zhou, Xu Runze, Lanqing Zhang, Siyuan Zhang: performed the  
409 investigation and analysed the samples. Zhou Chuanqiao and Peng Yu: wrote the  
410 original draft with major edits and inputs from Xu Xiaoguang, Zhang Limin and Wang  
411 Guoxiang.

412

#### 413 **Competing interests**

414 The authors declare that they have no known competing financial interests or  
415 personal relationships that could have appeared to influence the work reported in this  
416 paper.

417

#### 418 **Acknowledgements**

419 This work was supported by the National Natural Science Foundation of China  
420 (No.42077294, 41877336, 41971043), the Cooperation and Guidance Project of  
421 Prospering Inner Mongolia through Science and Technology (No.2021CG0037), the  
422 National Key Research and Development Program of China (No.2021YFC3200304),  
423 the Guangxi Key Research and Development Program of China (No.2018AB36010).

424

425 **References**

426 Amirbahman, A., Pearce, A.R., Bouchard, R.J., Norton, S.A., Kahl, J.S.: Relationship  
427 between hypolimnetic phosphorus and iron release from eleven lakes in Maine,  
428 USA, *Biogeochemistry*, 65(3), 369-385, 10.1023/A:1026245914721, 2003.

429 Anneville, O., Domaizon, I., Kerimoglu, O., Rimet, F., Jacquet, S.: Blue-Green algae  
430 in a “Greenhouse Century”? new insights from field data on climate change impacts  
431 on cyanobacteria abundance, *Ecosystems*, 18(3), 441-458, 10.1007/s10021-014-  
432 9837-6, 2015.

433 Azam, H.M., Finneran, K.T.: Fe(III) reduction-mediated phosphate removal as  
434 vivianite ( $\text{Fe}_3(\text{PO}_4)_2 \cdot 8\text{H}_2\text{O}$ ) in septic system wastewater, *Chemosphere*, 97, 1-9,  
435 100.1016/j.chemosphere.2013.09.032, 2014.

436 Baldwin, D.S., Mitchell, A.: Impact of sulfate pollution on anaerobic biogeochemical  
437 cycles in a wetland sediment, *Water Research*, 46(4), 965-974,  
438 10.1016/j.watres.2011.11.065, 2012.

439 Chen, M., Li, X.H., He, Y.H., Song, N., Cai, H.Y., Wang, C.H., Li, Y.T., Chu, H.Y.,  
440 Krumholz, L.R., Jing, H.L.: Increasing sulfate concentrations result in higher  
441 sulfide production and phosphorous mobilization in a shallow eutrophic freshwater  
442 lake, *Water Research*, 96, 94-104, 10.1016/j.watres.2016.03.030, 2016.

443 Chen, M., Ye, T.R., Krumholz, L.R., Jiang H.L.: Temperature and cyanobacteria bloom  
444 biomass influence phosphorous cycling in eutrophic lake sediments, *Plos One*, 9(3),  
445 e93130, 10.1371/journal.pone.0093130, 2014.

446 Cline, J.D.: Spectrophotometric determination of hydrogen sulfide in natural waters,  
447 *Limnology and Oceanography*, 14, 454-458, 1969.

448 Dierberg, F.E., DeBusk, T.A., Larson, N.R., Kharbanda, M.D., Chan, N., Gabriel, M.C.:  
449 Effect of sulfate amendments on mineralization and phosphorus release from South  
450 Florida (USA) wetland soils under anaerobic conditions, *Soil Biology &*  
451 *Biochemistry*, 43(1), 31-45, 10.1013/j.soilbio.2010.09.006, 2011.

452 Ebina, J., Tsutsui, T., Shirai, T.: Simultaneous determination of total nitrogen and total  
453 phosphorus in water using peroxodisulfate oxidation, *Water Research*, 17(12),  
454 1721-1726, 1983.

455 Fike, D.A., Bradley, A.S., Rose, C.V.: Rethinking the ancient sulfur cycle, *Annual*  
456 *Review of Earth and Planetary Science*, 43, 593-622, 10.1146/annurev-warth-  
457 060313-054802, 2015.

458 Friedrich, M.W., Finster, K.W.: How sulfur beats iron, *Science*, 344(6187), 974-975,  
459 10.1126/science.1255442, 2014.

460 Gu, S., Qian, Y.G., Jiao, Y., Li, Q.M., Pinay, G., Gruau, G.: An innovative approach  
461 for sequential extraction of phosphorus in sediments: Ferrous iron P as an  
462 independent P fraction, *Water Research*, 103, 352-361,  
463 10.1016/j.watres.2016.07.058, 2016.

464 Gunnars, A., Blomqvist, S.: Phosphate exchange across the sediment-water interface  
465 when shifting from anoxic to oxic conditions an experimental comparison of  
466 freshwater and brackish-marine systems, *Biogeochemistry*, 37(3), 203-226, 1997.

467 Guo, M.L., Li, X.L., Song, C.L., Liu, G.L., Zhou, Y.Y.: Photo-induced phosphate



468 release during sediment resuspension in shallow lakes: A potential positive  
469 feedback mechanism of eutrophication, *Environmental Pollution*, 258, 113679,  
470 10.1016/j.envpol.2019.113679, 2020.

471 Han, C., Ding, S.M., Yao, L., Shen, Q.S., Zhu, C.G., Wang, Y., Xu, D.: Dynamics of  
472 phosphorus-iron-sulfur at the sediment-water interface influenced by algae blooms  
473 decomposition, *Journal of Hazardous Materials*, 300, 329-337,  
474 10.1016/j.jhazmat.2015.07.009, 2015.

475 Hansel, C.M., Lentini, C.J., Tang, Y.Z., Johnston, D.T., Wankel, S.D., Jardine, P.M.:  
476 Dominance of sulfur-fueled iron oxide reduction in low-sulfate freshwater  
477 sediments, *The ISME Journal*, 9(11), 2400-2412, 10.1038/ismej.2015.50, 2015.

478 Ho, J.C., Michalak, A.M., Pahlevan, N.: Widespread global increase in intense lake  
479 phytoplankton blooms since the 1980s, *Nature* 574, 667-670, 10.1038/s41589-019-  
480 1648-7, 2019.

481 Holmer, M., Storkholm, P.: Sulphate reduction and sulphur cycling in lake sediments:  
482 a review, *Freshwater Biology*, 46, 431-451, 10.1046/j.1365-2427.2001.00687.x,  
483 2001.

484 Hsieh, Y.P., Shieh, Y.N.: Analysis of reduced inorganic sulfur by diffusion methods:  
485 improved apparatus and evaluation for sulfur isotopic studies, *Chemical Geology*,  
486 137(3), 255-261, 1997.

487 Iwayama, A., Ogura, H., Hiramata, Y., Chang, C.W., Hsieh, C.H., Kagami, M.:  
488 Phytoplankton species abundance in Lake Inba (Japan) from 1986 to 2016,  
489 *Ecological Research*, 32(6), 783-783, 10.1007/s11284-017-1482-z, 2017.

490 Jorgensen, B.B., Findlay, A.J., Pellerin, A.: The Biogeochemical sulfur cycle of Marine  
491 sediments, *Frontiers in Microbiology*, 10, 849, 10.3389/fmicb.2019.00849, 2019.

492 Liu, Z.S., Zhang, Y., Han, F., Yan, P., Liu, B.Y., Zhou, Q.H., Min, F.L., He, F., Wu,  
493 Z.B.: Investigation on the adsorption of phosphorus in all fractions from sediment  
494 by modified maifanite, *Scientific Reports*, 8, 15619, 10.1038/s41598-018-34144-w,  
495 2018.

496 Mao, Z.G., Gu, X.H., Cao, Y., Luo, J.H., Zeng, Q.F., Chen, H.H., Jeppesen, E.: How  
497 does fish functional diversity respond to environmental changes in two large  
498 shallow lakes? *Science of the total environment*, 753, 142158,  
499 10.1016/j.scitotenv.2020.142158, 2021.

500 Mort, H.P., Slomp, C.P., Gustafsson, B.G., Andersen, T.J.: Phosphorus recycling and  
501 burial in Baltic sea sediments with contrasting redox conditions, *Geochimica et*  
502 *Cosmochimica Acta*, 74(4), 1350-1362, 10.1016/j.gca.2009.11.016, 2010.

503 Melemdez-Pastor, I., Isenstein, E.M., Navarro-Pedreno, J., Park, M.H.: Spatial  
504 variability and temporal dynamics of cyanobacteria blooms and water quality  
505 parameters in Missisquoi Bay (Lake Champlain), *Water Supply*, 19(5), 1500-1506,  
506 10.2166/ws.2019.017, 2019.

507 Nakagawa, M., Ueno, Y., Hattori, S., Umemura, M., Yagi, A., Takai, K, Koba, K.,  
508 Sasaki, Y., Makabe, A., Yoshida, N.: Seasonal change in microbial sulfur cycling  
509 in monomictic Lake Fukami-ike, Japan, *Limnology and Oceanography*, 57(4), 974-  
510 988, 10.4319/lo.2012.57.4.0974, 2012.

511 Ni, Z.K., Wang, S.R., Wu, Y., Pu, J.: Response of phosphorus fractionation in lake

512 sediments to anthropogenic activities in China, *Science of the Total Environment*,  
513 699, 134242, 10.1016/j.scitotenv.2019.134242, 2020.

514 Pan, P., Guo, Z.R., Cai, Y., Liu, H.T., Wang, B., Wu, J.Y.: High-resolution imaging of  
515 labile P&S in coastal sediment: Insight into the kinetics of P mobilization associated  
516 with sulfate reduction, *Marine Chemistry*, 225, 103851, 10.1016/j.marchem.2020.  
517 103851, 2020.

518 Pester, M., Knorr, K.H., Friedrich, M.W., Wagner, M., Loy, A.: Sulfate-reducing  
519 microorganisms in wetlands-fameless actors in carbon cycling and climate change,  
520 *Frontiers in Microbiology*, 3(72), 10.3389/fmicb.2012.00072, 2012.

521 Phillips, E.J.P., Lovley, D.R.: Determination of Fe(III) and Fe(II) in Oxalate Extracts  
522 of Sediment, *Soil Science Society of America Journal*, 51: 938-941, 1987.

523 Roden, E.E.: Geochemical and microbiological controls on dissimilatory iron reduction,  
524 *Comptes Rendus Geoscience*, 338(6-7), 456-467, 10.1016/j.crte.2006.04.009, 2006.

525 Ruban, V., Lopez-Sanchez, J.F., Pardo, P., Rauret, G., Muntau, H., Quevauviller, P.:  
526 Harmonized protocol and certified reference material for the determination of  
527 extractable contents of phosphorus in freshwater sediments-A synthesis of recent  
528 works, *Fresenius J Anal Chem*, 370, 224-228, 10.1007/s002160100753, 2001.

529 Sela-Adler, M., Ronen, Z., Herut, B., Antler, G., Vigderovich, H., Eckert, W., Sivan,  
530 O.: Co-existence of Methanogenesis and sulfate reduction with common substrates  
531 in sulfate-rich estuarine sediments, *Frontiers in Microbiology*, 8(766),  
532 10.3389/fmicb.2017.00766, 2017.

533 Tabatabai, M.: A rapid method for determination of sulfate in water samples,

534 Environmental, 7, 237-243, 1974.

535 Taylor, K.G., Konhauser, K.O.: Iron in Earth surface systems: a major player in  
536 chemical and biological processes, Elements, 7(2), 83-87,  
537 10.2113/gselements.7.2.83, 2011.

538 Thamdrup, B., Dalsgaard, T., Jensen, M.M., Petersen, J.: Anammox and the marine N  
539 cycle, Geochimica et cosmochimica acta, 68(11), A325, 2004.

540 Wu, S.J., Zhao, Y.P., Chen, Y.Y., Dong, X.M., Wang, M.Y., Wang, G.X.: Sulfur  
541 cycling in freshwater sediments: A cryptic driving force of iron deposition and  
542 phosphorus mobilization, Science of the total environment, 657, 1294-1303,  
543 10.1016/j.scitotenv. 2018.12.161, 2019.

544 Xu, G.H., Sun, Z.H., Fang, W.Y., Liu, J.J., Xu, X.B., Lv, C.X.: Release of phosphorus  
545 from sediments under wave-induced liquefaction, Water Research, 144, 503-511,  
546 10.1016 /j.watres.2018.07.038, 2018.

547 Yan, X.C., Xu, X.G., Wang, M.Y., Wang, G.X., Wu, S.J., Li, Z.C., Sun, H., Shi, A.,  
548 Yang, Y.H.: Climate warming and cyanobacteria blooms: Looks at their  
549 relationships from a new perspective, Water Research, 125, 449-457,  
550 10.1016/j.watres.2017. 09.008, 2017.

551 Yu, T., Zhang, Y., Wu, F.C., Meng, W.: Six-Decade change in water chemistry of large  
552 freshwater lake Taihu, China, Environmental Science and Technology, 47(16),  
553 9093-9101, 10.1021/es401517h, 2013.

554 Zhang, S.Y., Zhao, Y.P., Zhou, C.Q., Duan, H.X., Wang, G.X.: Dynamic sulfur-iron  
555 cycle promoted phosphorus mobilization in sediments driven by the algae

556 decomposition, *Ecotoxicology*, 30(8), 1662-1671, 10.1007/s10646-020-02316-y,  
557 2020.

558 Zhao, Y.P., Wu, S.J., Yu, M.T., Zhang, Z.Q., Wang, X., Zhang, S.Y., Wang, G.X.:  
559 Seasonal iron-sulfur interactions and the stimulated phosphorus mobilization in  
560 freshwater lake sediments, *Science of the total environment*, 768, 144336,  
561 10.1016/j.scitotenv.2020.144336, 2021.

562 Zhao, Y.P., Zhang, Z.Q., Wang, G.X., Li, X.J., Ma, J., Chen, S., Deng, H., Annalisa  
563 O.H.: High sulfide production induced by algae decomposition and its potential  
564 stimulation to phosphorus mobility in sediment, *Science of the total environment*,  
565 650, 163-172, 10.1016/j.scitotenv.2018.09.010, 2019.

566 Zhou, C.Q., Peng, Y., Deng, Y., Yu, M.T., Chen, L., Zhang, L.Q., Xu, X.G., Zhao, F.J.,  
567 Yan, Y., Wang, GX.: Increasing sulfate concentration and sedimentary decaying  
568 cyanobacteria co-affect organic carbon mineralization in eutrophic lakes sediments,  
569 *Science of the total environment*, 2022, 806, 151260, 10.1016/j.scitotenv.2021.  
570 151260, 2022.